

---

## PICTORIAL ESSAY

---

# Sacrococcygeal Chordoma

MYS Soo, L Wong

Department of Radiology, Westmead Hospital, Sydney, Australia

### ABSTRACT

*The imaging findings in 5 cases of sacrococcygeal chordoma and 4 patients with other sacral tumours (1 primary neurogenic tumour, 1 metastatic tumour from primary disease in the breast and 1 from the kidney, and an abdominal paraganglioma) are presented to highlight features that may be peculiar to chordomas. Both chordomas and other sacral tumours show heterogeneous high signals on T2-weighted magnetic resonance imaging sequences and similar enhancement characteristics following intravenous contrast. In chordomas the appearance of numerous intralesional septations is distinguishing. On computed tomography, chordomas show characteristic calcification, and the size of the extrasacral soft tissue component can be seen to exceed the intraosseous counterpart. Magnetic resonance imaging is the imaging modality of choice in surgical planning and for long term management.*

*Key Words:* Chordoma, Magnetic resonance imaging, Surgery

### INTRODUCTION

Chordoma is a malignant tumour thought to arise from the notochordal rests. It is an uncommon tumour of the human skeleton, and has an incidence of 1% of all malignant bone neoplasms.<sup>1</sup> Approximately 50% of chordomas are sacrococcygeal in origin. Chordomas account for over 40% of all sacral tumours and should be included in the differential diagnosis of sacral tumour, particularly in the older age group.

Local invasiveness and destructiveness are characteristic features of the disease. The indolent nature and unpredictable behaviour of sacrococcygeal chordomas make early detection difficult. By the time the diagnosis is established, the tumour is usually very large. Complete surgical excision is the only therapeutic modality able to effect a cure.<sup>2</sup> Imaging techniques, in particular the excellent contrast resolution afforded by MRI, play a crucial role in surgical planning.<sup>3</sup> This paper presents the imaging features of 5 cases of sacrococcygeal chordoma managed at Westmead Hospital over the past

15 years and contrasts these findings with those of 4 patients with other sacral tumours.

### PATHOLOGY

Macroscopically, sacrococcygeal chordomas are usually well-demarcated by a pseudocapsule and range from 3 cm to 20 cm in diameter (median 8 cm).<sup>4</sup> Virtually all tumours involve bone, with extension into adjacent soft tissue and skeletal muscle. The cut surface of the tumour is characteristically soft, gelatinous, mucoid, and haemorrhagic. Occasional greyish-yellow, friable foci are observed, probably secondary to necrosis.

Characteristic histological features include a mixture of epithelioid and physaliferous cells. The latter are typically large with vacuolated cytoplasm and prominent vesicular nuclei. A sea of muco-myxoid material surrounds these cells. The tumour cells are frequently arranged into lobules, separated by fibrous tissues. Mitotic figures are scant or absent. Areas of cartilage and bone may be present.<sup>4</sup> These histopathological features form the basis of the variable and heterogeneous appearances shown in T1- and T2-weighted MRI sequences.

### APPLIED ANATOMY

Relevant anatomy is illustrated in Figure 1. The pelvic surface of the sacrum gives attachment to the piriformis

---

*Correspondence:* Dr. MYS Soo, Department of Radiology, Westmead Hospital, PO Box 533, Wentworthville, New South Wales 2145, Australia.

Tel: (61) 2 9845 6522; Fax: (61) 2 9687 2109;

Email: [rmso@imag.wsahs.nsw.gov.au](mailto:rmso@imag.wsahs.nsw.gov.au)

Submitted: 18 July 2001; Accepted: 28 January 2002.

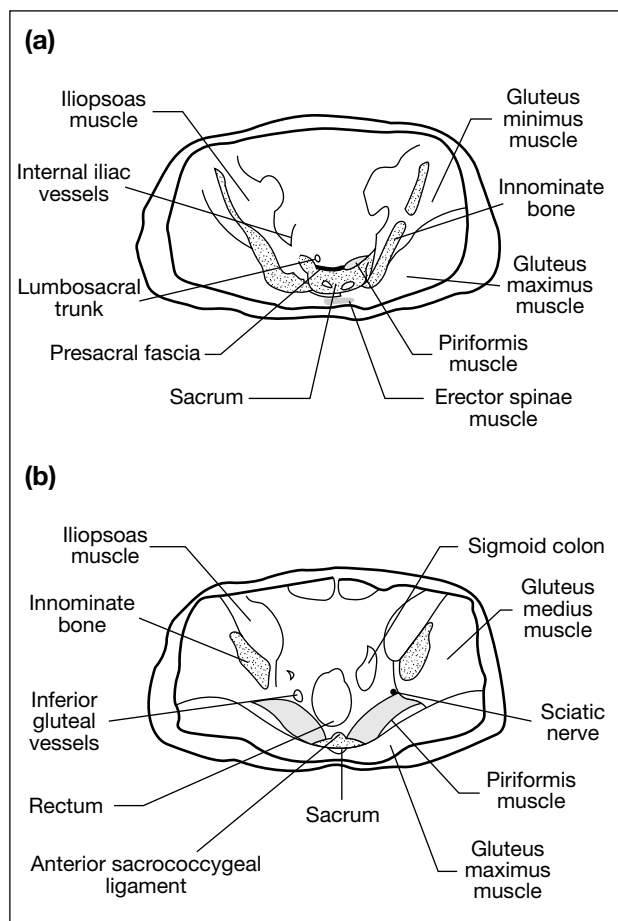


**Figure 1.** Diagrams of anatomy in the sacrococcygeal region. (a) An axial section through the pelvis at the S2/S3 level. Notice the proximity of the internal iliac vessels and the lumbo-sacral trunk to the lateral portion of the sacrum. The presacral fascia attaches firmly to the anterior sacrum; (b) an axial section at the lower S3 level. The piriformis and gluteus maximus muscles form the posterolateral wall of the pelvis. The sciatic nerve is anterior to the piriformis muscle prior to crossing into the gluteal region. The inferior gluteal branches of the internal iliac artery retain their retroperitoneal position.

muscles with the first three sacral ventral rami running along the anterior surface. The gluteus maximus muscles are inserted into the dorsal surfaces of the lower sacrum and the coccygeal body. The dorsal surface of the sacrum gives attachment to the erector spinae muscles.<sup>5</sup>

Situated at the root of the sigmoid mesentery and on either side of the midline are the paired internal iliac arteries and veins. In axial sections through the second sacral segment, the iliac vessels are medial to the iliopsoas muscles and anterior to the lumbo-sacral trunk.<sup>6</sup> Identification and clear definition of these structures is important, as the iliac arteries are ligated in the course of accessing the sacral tumour through a lower anterior abdominal surgical approach.

The presacral fascia is the caudal continuation of the anterior longitudinal ligament. Some of the terminal fibres of the anterior longitudinal ligament find attachment to the ventral surface of the first sacral body while others continue inferiorly as the anterior sacrococcygeal ligament.<sup>5</sup> The presacral fascia is described by Yonemoto et al<sup>7</sup> as a strong structure, resistant to tumour invasion. In sagittal T1-weighted images in normal subjects, it is shown as a thin uniform low signal intensity line between the sacrum and the rectum. The low signal of the fascia is due to its increased fibrous content.

## IMAGING FEATURES

The classical features of sacrococcygeal chordoma are that of a soft tissue mass with aggressive destruction of bone, and invasion of adjacent soft tissues and neurovascular structures in the pelvic cavity.<sup>1,8</sup> These features are pronounced in recurrent disease.<sup>1</sup> Posteriorly, the sacrospinalis and erector spinae muscles are commonly affected.

Intratumoural calcifications are observed on CT (Figure 2a) in almost 90% of cases.<sup>1,9</sup> On MRI, the lesion is of intermediate to low signal intensity in T1-weighted images and high intensity in T2-weighted images (Figure 2b). In T2-weighted sequences the lesions are usually of heterogeneous intensity caused by the presence of internal septations (Figure 2b). This unusual intralesional texture may also be highlighted in the T1-weighted scans following administration of intravenous contrast (Figure 3). The percentage of enhancement is variable and heterogeneous. The extent of advanced recurrent disease is best demonstrated by the excellent contrast resolution of MRI (Figure 4).

Although the morphology and the relation of these tumours to adjacent structures are shown best in T1-weighted sequences, proton density weighted images afford superior tissue contrast. The margins of the tumour, probably representing its pseudocapsule, are well-depicted (Figure 5a).

Occasional high signal areas in these neoplasms on T1-weighted MRI sequences may reflect high mucinous content or the presence of intratumoural haemorrhage (Figures 5b and 6a).<sup>10</sup> Sagittal images are useful in showing the exact origin of the tumour. While S4 and S5 (Figure 5b) are common sites of origin for a sacral chordoma,<sup>11</sup> another common site is the sacrococcygeal junction (Figure 6a). Very rarely a chordoma may have

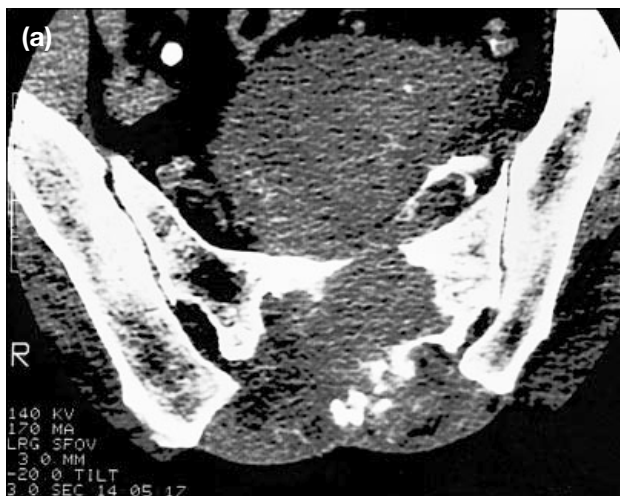


**Figure 2.** Imaging studies of a 65-year-old man on presentation with a 6-month history of constipation and a right sacral mass. (a) Axial CT through the second sacral segment shows a large bone-destroying soft tissue mass, with multiple foci of calcification. The lesion has eroded and enlarged the sacral canal and invaded the sacrospinalis and erector spinae muscles. Note the disproportionately large component of extrasacral tumour; (b) mid-line sagittal T2-weighted MRI scanning shows heterogeneous high signals within the mass. Intralésional septations are obvious. The still intact presacral fascia is displaced anteriorly (white arrows). The major portion of the chordoma was subsequently debulked using a posterior sacral approach.



**Figure 3.** Recurrent disease adjacent to the left sacral iliac joint is evident 3 years postsurgery. Axial T1-weighted contrast enhanced MRI shows heterogeneous but dense enhancement of the recurrent tumour. Note a small enhancing focus in the left innominate bone (white arrow) which could represent secondary metastasis. The posterior midline surgical scar shows a similar degree of enhancement (white arrowhead). The recurrent tumour was surgically debulked.



**Figure 4.** Sagittal T1-weighted MRI 4 years postsurgery. Further recurrent tumour is highlighted. Disease has now invaded the lower part of S1 and the upper sacral canal (black arrows). High signal streaks posteriorly (white arrowheads) may represent haemorrhagic foci.

an extrasosseous origin and show absent or minimal bony involvement.<sup>12, 13</sup> This is illustrated in Figure 6b in which a pelvic teratoma was initially suspected. A firm diagnosis of chordoma could only be established following an open biopsy. In this case, only certain sites

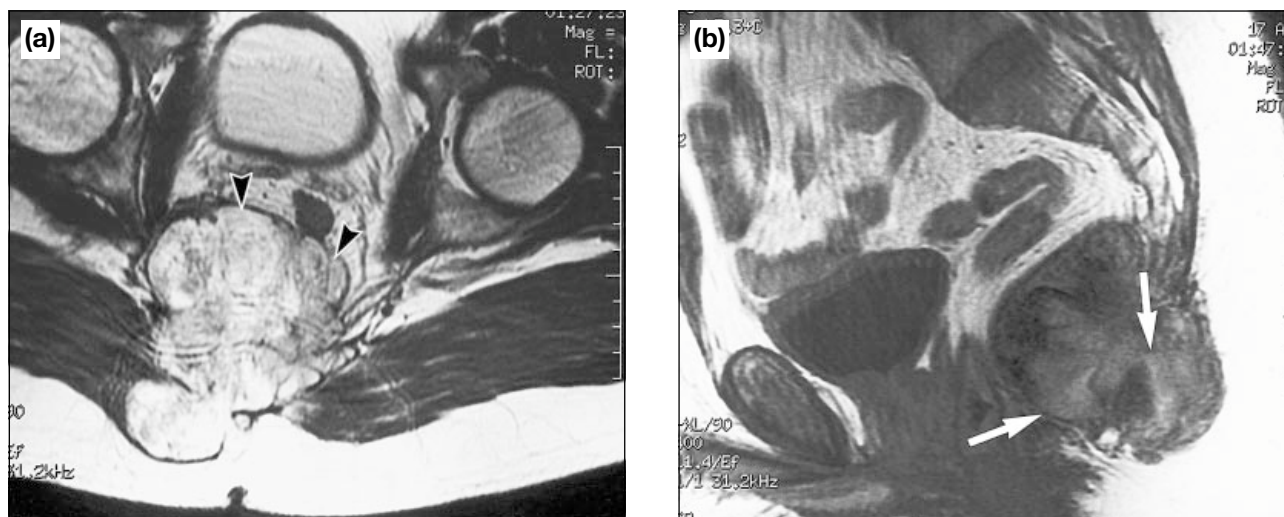


**Figure 5.** Imaging studies of a 41-year-old man with a 12 week history of an enlarging, slightly tender mass in the lower sacrum. (a) Axial proton density weighted MRI scan at the S4 level shows a well-defined tumour extending into the pelvic cavity. Note the obvious heterogeneous texture of the tumour caused by internal septations. Tumour invasion of the right gluteus maximus and obturator internus muscles is well-depicted. The thin curved low signal band (black arrowheads) probably represents tumour capsule; (b) midline sagittal T1-weighted MRI scan shows a well-defined low signal intensity mass, 6 cm in diameter, arising from the lower part of S4 and projecting anteroinferiorly. Intralesional high signals could be due to an increase in mucinous contents in the matrix (white arrows). Complete excision was performed using a combined lower abdominal-sacral surgical approach.

within the tumour show focal dense enhancement, but its invasion into the medial left gluteal muscles and adjacent subcutaneous tissues is distinctive (Figure 6c).

Intravenous contrast enhancement is less conspicuous on CT, not only in primary, but also in recurrent disease (Figure 7). Postsurgical scar tissues show the same degree of enhancement as tumour tissue on both CT (Figure 7) and MRI (Figure 3) images. The incidence of metastatic disease increases with multiple recurrent lesions.<sup>10</sup> Favoured sites of metastases include lung, lymph nodes, peritoneum, liver, and bone.<sup>1</sup> Multiple sites can be involved as seen in Figure 8. This patient had disease in the zygomatic arch and the thoracic spine.

Sacral chordomas require differentiation radiologically from rarer tumours which arise from the sacrum and emerging sacral nerve roots. These latter lesions may show similar signal and enhancement characteristics to sacral chordomas on MRI. A rare neurilemmoma with similar signal characteristics to sacral chordoma on T1- and T2-weighted images is illustrated in Figure 9. Note the lack of tumour internal septations in the sagittal T2-weighted images, however. The lesion's extrasacral component is no larger than its intrasacral portion — unusual for a chordoma — but the diagnosis was only certain in this case following an open biopsy. Similar diagnostic uncertainty arises with an intrasacral metastatic paraganglioma showing heterogeneous signals on T2-weighted images and irregular intralesional

signal voids. These signal voids are expressions of the tumour's vascularity (confirmed later on angiography). The almost total absence of extrasacral extension into pelvic soft tissue is uncharacteristic of a chordoma (Figure 10).

Solitary metastatic secondary deposits can show variable to dense enhancement on MRI but usually affect the first two sacral segments.<sup>14</sup> Lack of anterior pelvic soft tissue involvement and extensive intrinsic bone disease affecting the ala of the sacrum favour a diagnosis of metastatic deposits<sup>14</sup> (Figure 11). The presacral fascia also shows thin but definite contrast enhancement suggesting possible tumour infiltration (Figures 11 and 12).

## DISCUSSION

Sacrococcygeal chordomas, by virtue of their histological complexity, have some distinctive signal characteristics on MRI. The high protein content within the vacuolated vesicles of the physaliferous cells may account for the occasional bright signals seen on T1-weighted images. Internal septations noted are probably artefacts, caused by a mix of degraded blood products, calcification, necrosis, and the lobulated arrangement of the physaliferous and epithelioid cells marginated by fibrous tissue. This fibrous tissue, which is thought to form the walls of the internal septations and the pseudocapsule of the tumour, is often of low signal intensity on both T1- and T2-weighted images. The very

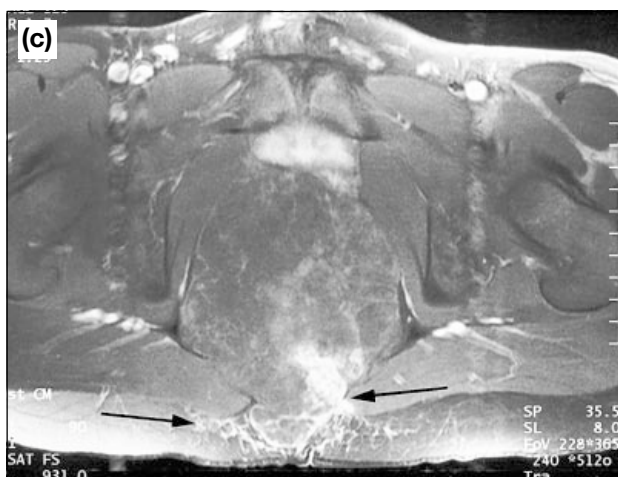
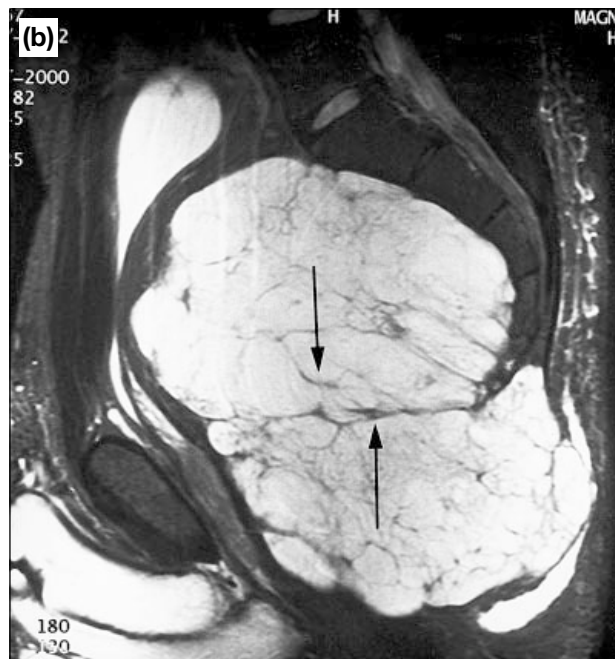
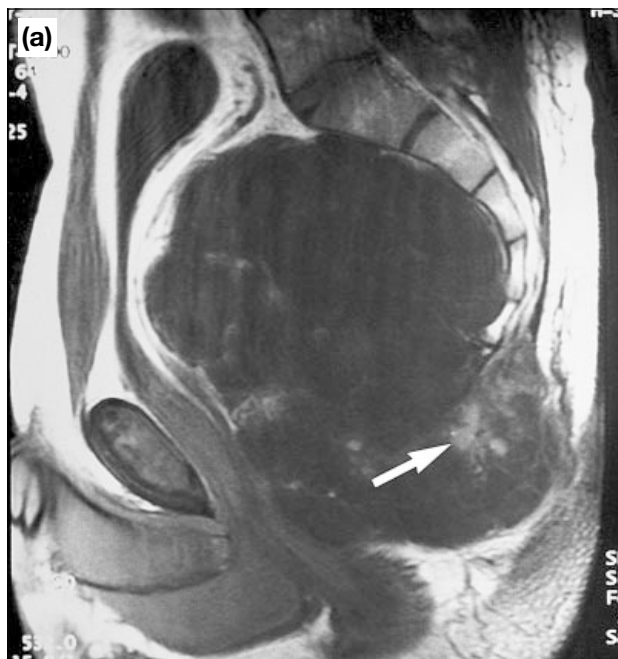


**Figure 6.** Imaging studies of an 18-year-old male presenting with progressive constipation and perineal pain of 16 weeks' duration. (a) Midline sagittal T1-weighted MRI shows a mixed signal, lobulated mass of 12 cm in diameter within the pelvic cavity. The mass appears to arise from the sacrococcygeal junction, with a moderate proportion projecting posteroinferiorly. Patchy high signals, probably representing mucinous content are seen (white arrow); (b) midline sagittal T2-weighted MRI shows the numerous internal septations that are the hallmark of chordomas (black arrows). However, because there was minimal bone involvement, a pelvic teratoma was also considered. Open biopsy showed features characteristic of chordoma — physaliferous cells with a lobulated arrangement, reinforced by numerous intratumoural fibrous septae; (c) contrast enhanced axial T1-weighted MRI at the level of the sacrococcygeal junction shows uneven contrast uptake by this large chordoma. Enhancement is most marked at the posterior margin, where muscle and subcutaneous tissue invasion is obvious (black arrows).

bright signals on T2-weighted sequences are thought to be due to the abundant fluid contents of vacuolated cells and the high protein and mucin within the tumour matrix.<sup>15</sup> An earlier report suggested that proton T1 and T2 values reflected the physical characteristics of intracellular and extracellular water, altered in malignancies through oedema formation and cellular disruption.<sup>16</sup>

The main conditions to consider in the differential diagnosis of an expansile lesion of the sacrum include a giant cell tumour, chondrosarcoma, ependymoma, plasmacytoma, and a solitary metastatic deposit.<sup>17, 18</sup> On MRI, these neoplasms may have similar signal characteristics to chordoma.<sup>11</sup> However, calcification on CT, origin at the sacrococcygeal junction, and the presence of internal septations are features that distinguish chordoma from other sacral neoplasms.<sup>1, 10, 14, 17</sup>

There is little correlation between the morphology of sacrococcygeal chordomas and their clinical course.<sup>2</sup> One study however, identified microscopic tumour necrosis and the presence of more than 5% Ki67 protein as adverse prognostic factors.<sup>2</sup> Since the first report by Meis et al,<sup>19</sup> the rare but highly malignant dedifferentiated variant of chordoma has been more frequently recognised and reported. Bergh et al<sup>2</sup> reported one chordoma with dedifferentiated features in their study of 39 chordomas of the sacrum and mobile spine, while Crapanzano et al<sup>20</sup> observed predominant pleomorphic sarcomatous cells in one case of dedifferentiated chordoma. These lesions are known to have a rapidly downhill clinical course due to early widespread secondary deposits.

The optimum curative treatment for sacrococcygeal chordoma is wide surgical resection leaving tumour



**Figure 7.** Contrast enhanced axial CT through recurrent tumour posterior to the second sacral segment in a 69-year-old man. Contrast uptake by the recurrent tumour is patchy and moderate (black arrowheads), as is contrast uptake of the posterior midline scar (white arrow).

free margins.<sup>2</sup> Due to frequent invasion of the neurovascular structures of the pelvis, complete surgical eradication of the tumour is often not possible. Adjuvant radiotherapy has proved successful in treating residual disease, particularly with regard to delaying recurrence.<sup>21, 22</sup> As illustrated in these cases and in the literature generally, a variety of surgical approaches can be used. The advent of high resolution CT and MRI has given surgeons more detailed information for planning surgery. The lower abdominal-sacral approach has recently regained popularity<sup>23</sup> although others still favour en bloc surgical removal.<sup>2</sup> When the lower abdominal-sacral approach is to be used, axial and coronal MRI sections can help identify the anatomy of vital structures, such as the rectum and the iliac veins and arteries. The latter are dissected free and ligated through an anterior lower abdominal approach to minimise bleeding and to help access the anterior part of the tumour prior to the second stage, which is a total excision of the chordoma from a posterior sacral approach.<sup>23</sup>



**Figure 8.** Imaging studies of a 69-year-old man presenting with recurrent sacral chordoma. (a) Midline sagittal T1-weighted MRI scan shows recurrent tumour in the second sacral body, with extension into the pelvic cavity (white arrow); (b) sagittal T1-weighted MRI scan. Note that metastatic disease has destroyed the posterior elements of T10, causing compression of the lower thoracic cord (black arrow).

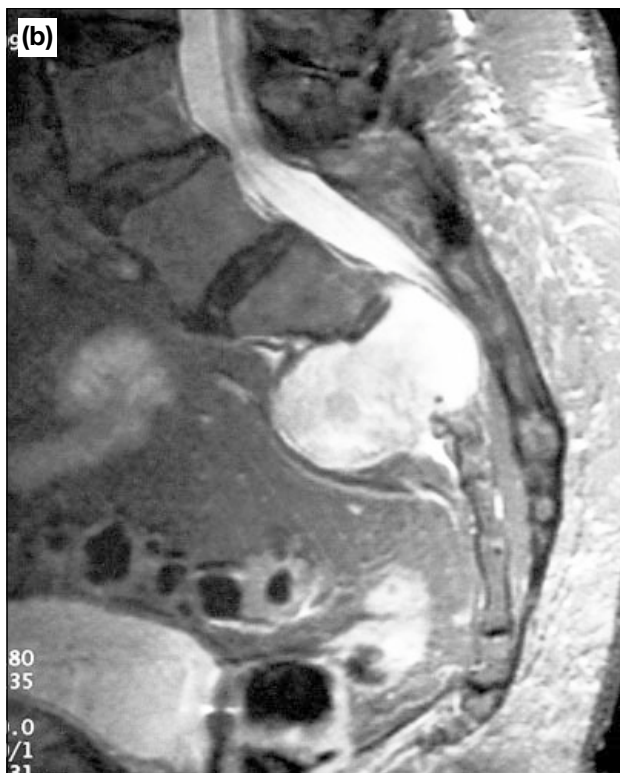
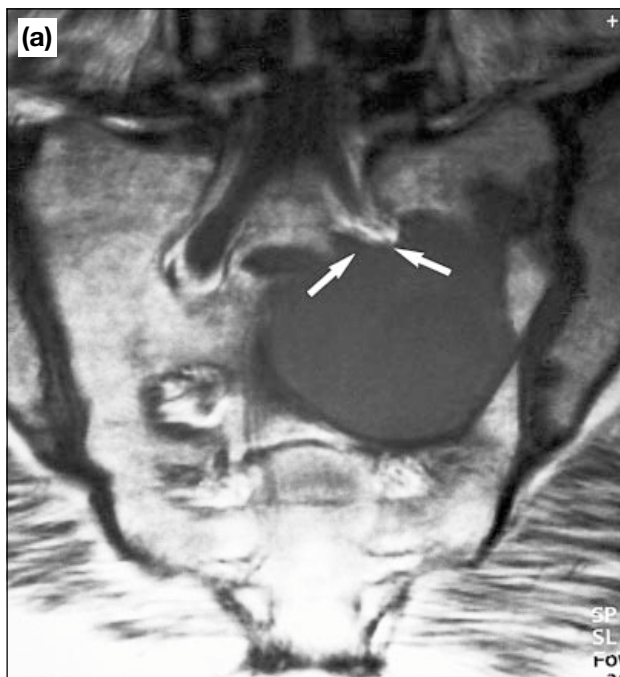


**Figure 9.** MRI scans of a 78-year-old woman presenting with a 2-year history of progressive pain and weakness in the left leg. (a) Coronal T1-weighted MRI scan through the body of the sacrum shows a well-defined low signal intrasacral tumour, 4.5 cm in diameter, which has destroyed S2 and extends cranially to involve the lower first sacral segment, amputating the left S1 root (white arrows); (b) sagittal T2-weighted MRI scan of the lesion shows high signals but a clear internal texture. The extrasacral portion of the tumour is equal in volume to its sacral component. Imaging features do not favour a chordoma although only an open biopsy was confirmatory of the tumour's neurogenic origin.



**Figure 10.** MRI scans of an 80-year-old woman with a confirmed histological diagnosis of metastatic paraganglioma of the first and second sacral segments. Note that the lesion is confined to the sacrum. (a) Axial T2-weighted section through S1 confirms its intrasacral position (black arrows) and shows numerous serpiginous signal voids which are a reflection of the tumour's increased vascularity; (b) coronal T1-weighted scan also demonstrates the serpiginous signal voids (white arrows).

## CONCLUSION

Imaging features of sacrococcygeal chordoma have been outlined. Sacrococcygeal chordomas must be differentiated from other primary sacral tumours and solitary metastasis, which typically arise from the first and second sacral segments. Chordomas arise from the lower three segments of the sacrum and the coccyx, destroying bone and invading soft tissue, usually extensively. The size of the soft tissue component of



**Figure 11.** MRI scans of a 46-year-old woman with secondary deposits in the sacrum from a primary breast carcinoma. (a) Contrast enhanced axial T1-weighted MRI shows uniform enhancement in the whole body of the expanded first sacral segment, including the ala. The posterior portion encroaches on the sacral canal. Note the thin but definite enhancement of the presacral fascia (white arrows); (b) sagittal T1-weighted MRI section shows the bodies of both S1 and S2 to be affected.



**Figure 12.** Contrast enhanced sagittal T1-weighted MRI of a 60-year-old man with renal cell carcinoma and metastatic deposits in the bodies of S1, S2 and S3. Note the extensive bone destruction. The region anterior to the sacrum at S3 shows slight bulging, with interruption of the low signal presacral fascia suggesting probable breach of this structure (white arrow).

the tumour usually exceeds its intraosseous counterpart. Imaging findings of a bone-eroding and contrast-enhancing, calcified soft tissue mass arising from S4, S5 or the sacrococcygeal junction is strongly suggestive of chordoma.

## ACKNOWLEDGEMENTS

The authors thank Ms L Spooner and the staff of the Audio-Visual Department at Westmead Hospital for their assistance.

## REFERENCES

1. Smith J, Ludwig RL, Marcove RC. Sacrococcygeal chordoma: A clinicoradiological study of 60 patients. *Skeletal Radiol* 1987; 16:37-44.
2. Bergh P, Kindblom LG, Gunterberg B, et al. Prognostic factors in chordoma of sacrum and mobile spine: A study of 39 patients. *Cancer* 2000;88:2122-2134.
3. Ramsay RG. Teaching atlas of spine imaging. New York: Thieme Medical Publications; 1999:256-257.
4. Rosai J. Bones and joints. In: Rosai J, Ackerman LV, eds. *Ackermann's surgical pathology*. 8th ed. St Louis: Mosby Year Book; 1996:1971-1973.
5. Warwick R, Williams PL. Osteology. In: Gray H. *Gray's anatomy*. 35<sup>th</sup> ed. Edinburgh: Longman; 1973:242-245.
6. Gilbert TJ. Male pelvis. In: El-Khoury GY, Montgomery WJ, Bergman RA. *Sectional anatomy by MRI*. 2nd ed. New York: Churchill Livingstone; 1995:504-506
7. Yonemoto T, Tatzaki S, Takenouchi T, Ishii T, Satoh T, Moriya H. The surgical management of sacrococcygeal chordoma. *Cancer* 1999;85:878-883.

8. Meyer JE, Lepke RA, Lindfors KK et al. Chordomas: their CT appearance in the cervical, thoracic and lumbar spine. *Radiology* 1984;153:693-696.
9. Krol G, Sundaresan N, Deck M. Computed tomography of axial chordomas. *J Comput Assist Tomogr* 1983;7:286-289.
10. St Amour TE, Hodges SC, Langman RW, Tamas DE. Chordoma. In: St Amour TE, Hodges SC. *MRI of the spine*. New York: Raven Press; 1994:475-481.
11. Wetzel LH, Levine E. MR Imaging of sacral and presacral lesions. *AJR Am J Roentgenol* 1990;154:771-775.
12. Sundaresan N. Chordoma. *Clinical Orthop* 1986;204:135-142.
13. Tomlinson FH, Scheithauer BW, Miller GM, Onofrio BM. Extraosseous spinal chordoma. *J Neurosurg* 1991;75:980-984.
14. Dietemann JL, Caille JM, Manelfe C, Clarisse J, Railhac JJ. The sacrum: normal and pathological aspects. In: Manelfe C, ed. *Imaging of spine and spinal cord*. New York: Raven Press; 1992: 790-792.
15. Weber AL, Liebsch NJ, Sanchez R, Sweriduk ST Jr. Chordomas of the skull base: radiologic and clinical evaluation. *Neuroimaging Clin N Am* 1994;4:515-527.
16. Rosenthal DI, Scott JA, Mankin HJ, Wismer TL, Brady TJ. Sacrococcygeal chordoma: magnetic resonance imaging and computed tomography. *AJR Am J Roentgenol* 1985;145:143-147.
17. Resnick D. *Diagnosis of bone and joint disorders*. 3rd ed. Philadelphia: WB Saunders Co; 1995:3846-3854.
18. Stewart D, Price P. Indolent plasmacytoma. *Australas Radiol* 2001;45:531-533.
19. Meis JM, Raymond AK, Evans HL, Charles RE, Giraldo AA. "Dedifferentiated" chordoma. A clinicopathologic and immunohistochemical study of three cases. *Am J Surg Pathology* 1987; 11:516-25.
20. Crapanzano JP, Ali SZ, Ginsberg MS, Zokowsk MF. Chordoma: A cytologic study with histologic and radiologic correlation. *Cancer* 2001;93:40-51.
21. Keisch ME, Garcia DM, Shibuya RB. Retrospective long-term follow-up analysis in 21 patients with chordomas of various sites treated at a single institution. *J Neurosurg* 1991;75:374-377.
22. York JE, Kaczaraj A, Abi-Said D, et al. Sacral chordoma: 40 year experience at a major cancer center. *Neurosurgery* 1999; 44:74-80.
23. Chandawarkar RY. Sacrococcygeal chordoma: review of 50 consecutive patients. *World J Surg* 1996;20:717-719.